HHS Public Access

Author manuscript

Proc SPIE Int Soc Opt Eng. Author manuscript; available in PMC 2017 February 27.

Published in final edited form as:

Proc SPIE Int Soc Opt Eng. 2016 February 27; 9788: . doi:10.1117/12.2216558.

A semi-automatic framework of measuring pulmonary arterial metrics at anatomic airway locations using CT imaging

Dakai Jin[a], **Junfeng Guo**[b,c], **Timothy M. Dougherty**[b,c], **Krishna S. Iyer**[b,c], **Eric A. Hoffman**[b,c], and **Punam K. Saha**[*,a,c]

[a]Dept. of Electrical and Computer Engineering, University of Iowa, Iowa City, IA, USA

[b]Dept. of Biomedical Engineering, University of Iowa, Iowa City, IA, USA

[c]Dept. of Radiology, University of Iowa, Iowa City, IA, USA

Abstract

Pulmonary vascular dysfunction has been implicated in smoking-related susceptibility to emphysema. With the growing interest in characterizing arterial morphology for early evaluation of the vascular role in pulmonary diseases, there is an increasing need for the standardization of a framework for arterial morphological assessment at airway segmental levels. In this paper, we present an effective and robust semi-automatic framework to segment pulmonary arteries at different anatomic airway branches and measure their cross-sectional area (CSA). The method starts with user-specified endpoints of a target arterial segment through a custom-built graphical user interface. It then automatically detect the centerline joining the endpoints, determines the local structure orientation and computes the CSA along the centerline after filtering out the adjacent pulmonary structures, such as veins or airway walls. Several new techniques are presented, including collision-impact based cost function for centerline detection, radial sample-line based CSA computation, and outlier analysis of radial distance to subtract adjacent neighboring structures in the CSA measurement. The method was applied to repeat-scan pulmonary multirow detector CT (MDCT) images from ten healthy subjects (age: 21–48 Yrs, mean: 28.5 Yrs; 7 female) at functional residual capacity (FRC). The reproducibility of computed arterial CSA from four airway segmental regions in middle and lower lobes was analyzed. The overall repeat-scan intra-class correlation (ICC) of the computed CSA from all four airway regions in ten subjects was 96% with maximum ICC found at LB10 and RB4 regions.

Keywords

Pulmonary artery; airway tree; computed tomography; minimum cost path; radial sample line; cross sectional area

1. INTRODUCTION

Pulmonary vascular dysfunction is gaining increased attention in regards to the role played in the development and progression of smoking associated parenchymal destruction

* pksaha@engineering.uiowa.edu.

(emphysema).[1–5] Pulmonary arterial enlargement, measured using multirow detector CT (MDCT) imaging, has recently been established to be an important predictor of functional lung decline and morbidity in COPD patients.[4, 5] Matsuoka[6] reported decreased cross-sectional area of pulmonary peripheral vessels in patients with COPD in relation to increased emphysema and airway flow limitations. Results of these studies suggest the importance of analyzing the pulmonary arterial morphology for early detection of pulmonary diseases, understanding their etiologies, and evaluating and monitoring the treatment effects.

Although, early attempts of measuring pulmonary arterial morphology date back to the beginning of volumetric CT,[7] Standardized framework for measuring arterial morphological metrics associated to different anatomic lung regions is missing. The major challenges originate from the lack of a robust approach to identify associated pulmonary arteries in either intra- or inter-subjects, due to the geometric and topologic complexity of the pulmonary vascular tree, especially in the presence of artery, vein, and airway wall fusion from partial volume effects, and the heart motion effects from CT imaging. These challenges limited the previous studies[4–6] only to aorta or small peripheral vascular regions. Few works[8, 9] had been attempted to automatically segment the entire pulmonary arterial trees, but with very limited results. Recently, Jin, et. al.[10, 11] developed a fully automatic algorithm to segment and quantify pulmonary arteries associated to anatomically defined airway branches by exploring the unique pairing[12] between arterial and airway branches that is established by their spatial proximity and parallel configuration. However, the accuracy of the method needs to be further improved to approach practical clinical studies. Therefore, there is an urgent need to develop an effective and robust method to standardize the quantification of the arterial morphology associated to anatomic lung regions that is suitable for analysis of the intra- or inter-subjects.

Toward this goal, we present a semi-automatic framework to segment pulmonary arteries at anatomic airway regions and measure their cross-sectional area (CSA), which aims to serve as a practical tool for large cross-sectional and longitudinal research and clinical studies. The method was applied to repeat-scan pulmonary MDCT images from ten healthy subjects (age: 21–48 Yrs, mean: 28.5 Yrs; 7 female) at functional residual capacity (FRC). The reproducibility of computed arterial CSA from four airway segmental locations in middle and lower lobes was analyzed, and the results are reported.

2. METHODS

The purpose of the method design was to build an efficient semi-automatic tool for measuring pulmonary arterial that is minimal in user-interaction, robust, and the measured metrics are linked to consistent anatomic lung locations that can be translated to large cross-sectional and longitudinal studies. The method utilizes the fact of pulmonary anatomy [12] that airway and arterial branches has a unique pairing that is established by their spatial proximity and parallel configuration. In fact, radiologists have long used this pairing as a means of identifying abnormal airway or arterial dimensions such as the “signet” sign[13] used to identify bronchiectasis. Specifically, the method starts with user-specified end-points of a target arterial segment associated to a specific airway anatomic branch through a

custom-built graphical user interface (GUI). Subsequently, it automatically detects the centerline joining the end-points of the user-specified arterial segment, determines the local structure orientation along the centerline and computes the CSA along the centerline after filtering out the adjacent pulmonary structures, such as airway walls or veins. Among those, several new techniques are presented, including collision-impact based cost function for centerline detection, radial sample-line based CSA computation, and outlier analysis of radial distance to subtract adjacent neighboring structures in the CSA measurement.

The entire method is accomplished in the following sequential steps—(1) segmentation of vascular structures from CT images,[14, 15] (2) segmentation and labeling of the airway from CT images,[16, 17] (3) user-specification of arterial endpoints associated to a target airway branch, e.g., RB4 and RB10, (4) tracing of the centerline for the user-specified arterial segment, (5) computation of local arterial orientation along the centerline, and (6) computation of arterial CSA after subtracting the adjacent pulmonary structures. See the schematic illustration in Figure 1.

Section 2.1 Preprocessing of the pulmonary CT images

The method first segments the pulmonary vascular structures from CT images[14, 15] (Figure 1.(b)). Due to the intensity similarity, it is difficult to automatically separate the artery and vein trees from non-contrast CT images. Therefore, the whole vascular structure, containing both artery and vein trees, is used as input to the following user-specification and centerline tracing steps. Then, the airway tree is segmented and anatomically labeled from CT images[16, 17] (Figure 1.(b)). In contrast to the geometric and topologic complexity of vascular structures, the airway trees possess simpler and more consistent branching patterns and standardized anatomic nomenclatures that are available up to several generational or segmental levels. Therefore, the airway tree provides a robust benchmark to identify consistent arterial branches associated to different lung regions, which is suitable for cross-sectional and longitudinal studies.

Section 2.2 User-specification of the matching arterial endpoints

The preprocessing step provides the anatomically labeled airway tree, which serves as the reference for the expert to identify the matching arterial segment associated to specific airway branch through a custom built GUI. The airway branch at interested lung region, e.g. LB9, is first highlighted with color. Then, based on the spatial proximity and parallel configuration between arterial and airway branches, the expert browses through the 2-dimensional slices to identify the matching arterial segment associated with specific airway branch,. The expert may need to trace all the way back to the main pulmonary artery or trace down to peripheral vessels to confirm a true arterial segment. After confirming, two endpoints will be manually placed near the starting and ending locations of the matching arterial segment through the GUI. Figure 1.(c) shows a coronal view of the CT image at the airway branch of LB9 and the user specified two arterial end-voxels (marked by blue cross).

Section 2.3 Tracing of arterial centerline

After user-specification of the two endpoints of the matching arterial segment at specific airway location, a centerline connecting the two arterial endpoints is generated, which is

necessary for the orientation determination and the CSA computation in the later steps. To generate an accurate centerline connecting two endpoints, a minimum-cost path approach[18] was applied. Here, a medialness measure called *collision impact*[19] was used to define the cost function to impose the centerness of a path. The collision impact captures the degree of medialness for a point in the object. Based on the gradient map of the fuzzy distance transform[20] of the vascular structures, collision impact at a given voxel p in fuzzy object $\mathcal{O}$, denoted by $\xi(p)$, is defined as follow:

$$\xi(p)=1-\max_{q\in N_{26}^{*}(p)}\frac{f_{+}\left(FDT(q)-FDT(p)\right)}{\frac{1}{2}\left(f_{\mathcal{O}}(p)+f_{\mathcal{O}}(q)\right)|p-q|}, \quad (1)$$

where $FDT(\cdot)$ give the fuzzy distance transform, $f_{\mathcal{O}}: Z^3 \rightarrow [0, 1]$ is the membership function, $N_{26}^{*}(\cdot)$ is the 26-neighborhood, and $f_{+}(x)$ returns the value of x if $x > 0$ and zero otherwise. It can be shown that collision impact at a given object voxel lies in the interval [0,1]. Voxels within the central region of a shape will take the value close to '1', while it takes the value close to '0' at non-central voxels. Results of the fuzzy distance transform and the collision impact value are illustrated in Figure 2(b) and Figure 2(c), respectively.

The collision impact measure is used to define the path cost. A path π is an ordered sequence of voxels where every two successive voxels are 26-adjacent, i.e., $\pi = \langle p_0, p_1, \cdots, p_{l-1}\rangle$ where $p_{i-1}, p_i \in Z^3$ are 26-adjacent for every $i = 1, \cdots, l-1$. Total path cost is defined by adding the cost of individual discrete steps between every two successive voxels on the path. The *step-cost function*[21] of a discrete step between two 26-adjacent voxels $p, q \in Z^3$ is defined as follows:

$$cost(p,q)=\frac{|p-q|}{\varepsilon+\left(\text{average}(\xi(p),\xi(q))\right)^2}, \quad (2)$$

where the parameter ε is a small number used to overcome numerical computational difficulties. Results of the step-cost map are illustrated in Figure 2(d). Finally, the minimum-cost path connecting the two user-specified arterial endpoints may be computed using a dynamic programming algorithm. See Figure 3(b) for the arterial centerline detection results at the airway branch of RB10 on a CT data.

Section 2.4 Computation of arterial CSA

After computation of the arterial centerline, the arterial CSA at every centerline location p is computed as follows. First, the local arterial orientation at p is determined using the principal component analysis (PCA) of centerline voxels around p. Then, the interpolated object representation on an orthogonal plane through p is generated (Figure 1(d)) using tri-linear interpolation. The arterial CSA then is computed at every centerline point and the average of CSA measures at the central half points is used as the arterial CSA measure for an arterial segment.

A radial sample line approach was used to compute the arterial CSA. Initial estimate of the vessel boundary is determined on the orthogonal plane through the center location by casting a set of radial sample lines[22], and full-width half-max criterion is applied for the computation of edge location (Figures 1(d) and 3(c)). In the next step, the influence of adjacent neighboring structure on initial vessel boundary is eliminated using an outlier analysis on radial distance distribution $\langle d_1, d_2, \cdots, d_N \rangle$ of initial edge locations (Figures 1(e,f) and 3(d,e)). Let $\tilde{d}$ denote the median of the radial distance values, and let be σ_d standard deviation of the distance values $d_i \leq \tilde{d}$. An edge point at a distance greater that $\tilde{d} + 3\sigma_d$ is eliminated as an incorrect vessel edge point, and the new edge point on the corresponding radial line is located using the reference of correct edge points with $d_i \leq \tilde{d} + 3\sigma_d$ on nearest sample lines on both sides; see green dots on Figure 1(f)). Figure 3(d,e) illustrates the performance of outlier elimination of the vessel boundary on an CT data associated to airway branch of RB10. Finally, the CSA is computed using the polygonal representation of vessel boundary after outlier correction.

3. RESULTS

The experiments were aimed to examine the reproducibility of the new framework for the arterial CSA measurement associated to different lung regions. The method was applied on repeat MDCT scans of ten normal non-smoking subjects (Previously acquired under IRB approval; age: 21–48 Yrs, mean: 28.5 Yrs; 7 female) at functional residual capacity (FRC: 20% vital capacity). MDCT scans were acquired on a Siemens Definition Flash 128 (at 120kV with effective mAs of 200), and the images were reconstructed at 0.5mm slice thickness using a standard B35 kernel. The second repeat scan was acquired at a time gap of 3–5 minutes.

Reproducibility of the method was examined by computing intra-class correlation (ICC) of CSA measures in repeat MDCT scans. For each lung image, CSA measures were computed over four anatomic airway branches—RB4, RB10, LB4 and LB10. The results of the reproducibility and the observed values (mean±std.) of arterial CSA measures are summarized in Table 1. The overall ICC of arterial CSA measures from all the four airway paths was 96%. Among the four paths, the lowest reproducibility was observed at LB4, which may be caused by the influence of cardiogenic motion over that lung region. In general, higher reproducibility of CSA measures were found in lower lung lobes.

4. DISCUSSIONS AND CONCLUSIONS

This paper presents an efficient semi-automatic framework for segmentation of pulmonary arteries at different anatomic airway branches and measurement of arterial morphological metrics, the cross-sectional area (CSA), which may serve as a practical tool for large cross-sectional and longitudinal clinical studies. Although it is challenging to automatically identify the associated arterial segments, due to the complexity of pulmonary vascular tree, especially in the presence of artery, vein, and airway wall fusion, and the heart motion effects, the problem can be solved by the expert interaction based on the spatial proximity and parallel configurations uniquely characterized between the pulmonary arterial and airway branches. The accurate arterial CSA computation is achieved using several new

techniques presented in this paper, including collision-impact based cost function for arterial centerline detection, radial sample-line based CSA computation, and the outlier analysis of radial distance to subtract adjacent neighboring structures in CSA measurement, such as veins or airway walls.

Repeat scan MDCT reproducibility study on ten normal human subjects has shown that the methods can produce arterial CSA values at airway regions of LB10 and RB4 with high repeatability. The entire process for each airway branch required 2–3 minutes to complete, including user interaction through GUI and the automated steps to complete CSA computation. Since there are four airway branches measured in this study, it took about 10 minutes to process one dataset. Currently, we are performing a comprehensive study evaluating the accuracy and robustness of this framework in a larger human study group.

Acknowledgments

This work was supported by the NIH grant R01 HL112986.

References

1. Santos S, Peinado VI, Ramirez J, et al. Characterization of pulmonary vascular remodelling in smokers and patients with mild COPD. Eur Respir J. 2002; 19(4):632–638. [PubMed: 11998991]
2. Alford SK, van Beek EJ, McLennan G, et al. Heterogeneity of pulmonary perfusion as a mechanistic image-based phenotype in emphysema susceptible smokers. Proceedings of the National Academy of Sciences. 2010; 107(16):7485–7490.
3. Barr RG, Bluemke DA, Ahmed FS, et al. Percent emphysema, airflow obstruction, and impaired left ventricular filling. N Engl J Med. 2010; 362(3):217–227. [PubMed: 20089972]
4. Wells JM, Washko GR, Han MK, et al. Pulmonary arterial enlargement and acute exacerbations of COPD. N Engl J Med. 2012; 367(10):913–921. [PubMed: 22938715]
5. Wells JM, Dransfield MT. Pathophysiology and clinical implications of pulmonary arterial enlargement in COPD. Int J Chron Obstruct Pulmon Dis. 2013; 8:509–521. [PubMed: 24235822]
6. Matsuoka S, Washko GR, Dransfield MT, et al. Quantitative CT measurement of cross-sectional area of small pulmonary vessel in COPD: correlations with emphysema and airflow limitation. Acad Radiol. 2010; 17(1):93–99. [PubMed: 19796970]
7. Liu YH, Hoffman EA, Ritman EL. Measurement of three-dimensional anatomy and function of pulmonary arteries with high-speed x-ray computed tomography. Invest Radiol. 1987; 22(1):28–36. [PubMed: 3102399]
8. Pisupati C, Wolff L, Mitzner W, et al. Tracking 3-D pulmonary tree structures. Proc of the Workshop on Math Methods in Biomed Image Anal. 1996:160–169.
9. Bulow T, Wiemker R, Blaffert T, et al. Automatic extraction of the pulmonary artery tree from multi-slice CT data. SPIE: Medical Imaging. 2005; 5746:730–740.
10. Jin D, Iyer KS, Hoffman EA, et al. Reconstruction Of Pulmonary Central Artery Volume In MDCT Imaging Using Airway Correspondence At Different Anatomic Branches. Am J Respir Crit Care Med. 2014; 189:A4311.
11. Jin D, Iyer KS, Hoffman EA, et al. Automated assessment of pulmonary arterial morphology in multi-row detector CT imaging using correspondence with anatomic airway branches. Proc of 11th Intern Symp on Visual Computing (ISVC), LNCS. 2014; 8887:521–530.
12. Singhal S, Henderson R, Horsfield K, et al. Morphometry of the human pulmonary arterial tree. Circ Res. 1973; 33(2):190–197. [PubMed: 4727370]
13. Marshall GB, Farnquist BA, MacGregor JH, et al. Signs in thoracic imaging. J Thorac Imaging. 2006; 21(1):76–90. [PubMed: 16538167]

14. Shikata H, McLennan G, Hoffman EA, et al. Segmentation of pulmonary vascular trees from thoracic 3D CT images. Journal of Biomedical Imaging. 2009; 2009:24.
15. Saha PK, Udupa JK, Odhner D. Scale-based fuzzy connected image segmentation: theory, algorithms, and validation. Computer Vision and Image Understanding. 2000; 77:145–174.
16. Tschirren J, Hoffman EA, McLennan G, et al. Intrathoracic airway trees: segmentation and airway morphology analysis from low-dose CT scans. IEEE Trans Med Imaging. 2005; 24(12):1529–1539. [PubMed: 16353370]
17. Tschirren J, McLennan G, Palagyi K, et al. Matching and anatomical labeling of human airway tree. IEEE Trans Med Imaging. 2005; 24(12):1540–1547. [PubMed: 16353371]
18. Saha P, Strand R, Borgefors G. Digital topology and geometry in medical imaging: a survey. IEEE Transactions on Medical Imaging. 2015; 34(9):1940–1964. [PubMed: 25879908]
19. Jin D, Chen C, Saha PK. Filtering Non-Significant Quench Points Using Collision Impact in Grassfire Propagation. Proc of 18th Intern Conf on Image Anal and Process (ICIAP), LNCS. 2015; 9279:432–443.
20. Saha PK, Wehrli FW, Gomberg BR. Fuzzy distance transform: theory, algorithms, and applications. Computer Vision and Image Understanding. 2002; 86:171–190.
21. Jin D, Iyer KS, Chen C, et al. A robust and efficient curve skeletonization algorithm for tree-like objects using minimum cost paths. Pattern Recognition Letters. 2015 in press.
22. Liu Y, Jin D, Li C, et al. A robust algorithm for thickness computation at low resolution and its application to in vivo trabecular bone CT imaging. IEEE Transactions on Biomedical Engineering. 2014; 61(7):2057–2069. [PubMed: 24686226]

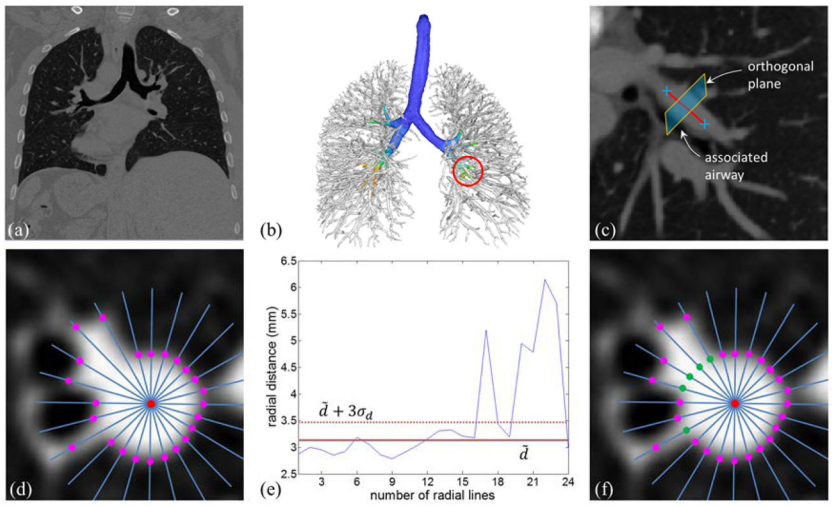

Figure 1.

Schematic illustration of the working process of our proposed framework. (a) A coronal view of lung MDCT image, (b) segmented and labeled airway tree overlapped with segmented vascular tree, (c) a zoomed in coronal view of the CT image at the airway branch of LB9 and the user specified two arterial endpoints and the centerline joining them. (d–e) Illustration of the CSA computation with the outlier analysis based on a radial ample line approach on the orthogonal plane cut in (c). (d) 2D orthogonal plane with the initial edge locations determined using half-max criterion. Central point (red), example of 24 sample lines (blue), initial edge locations(pink); (e) outlier analysis of the radial distance distribution, which eliminated incorrect sample lines touching the adjacent structures; (f) new edge locations are marked in green.

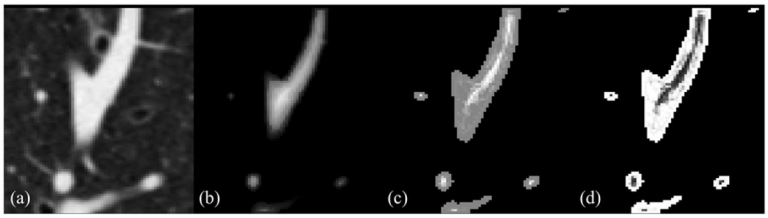

Figure 2.

Illustration of the collision impact and step-cost functions on a small region in a 2-D coronal view of a pulmonary CT image. (a) A small region from an original CT image slice. (b) Fuzzy distance transform of the vascular structures. (c) Collision impact values. (d) Path cost functions.

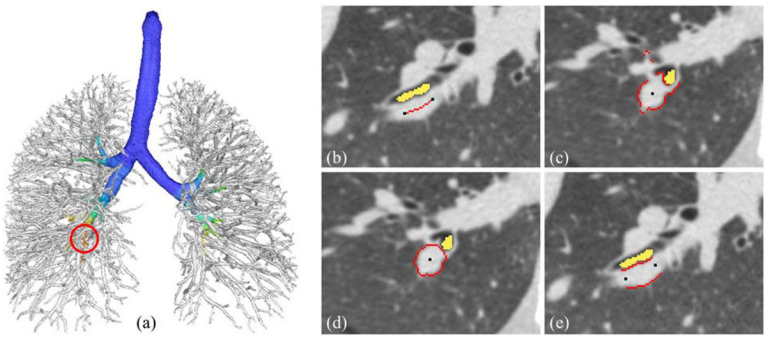

Figure 3.

Example of the intermediate results of the arterial centerline tracing and its CSA computation using proposed method at the airway branch of RB10 (a). (b) Coronal plane of the user specified two arterial end-voxels with the minimum-cost path connecting them; (c) the initial edge locations in the transverse plane determined using half-max criterion; (d,e) the new edge locations after outlier analysis of the radial distance in the transverse (d) and coronal (e) plane.

Table 1

Intra class correlation (ICC) and the observed values of CSA measures at four anatomic airway paths in repeat MDCT scans of ten subjects at functional residual capacity (FRC: 20% vital capacity).

	RB4	RB10	LB4	LB10
ICC	97%	92%	83%	98%
Observed values (mean±std.) (mm^2)	18.8 ± 5.7	44.2 ± 23.6	21.4 ± 4.0	39.3 ± 10.8